Data in Brief 53 (2024) 110138

Contents lists available at ScienceDirect

Data in Brief

journal homepage: www.elsevier.com/locate/dib

Data Article

Data on searching for synergy between alcohol and salt to produce more potent and environmentally benign gas hydrate inhibitors

Anton P. Semenov[a,*], Rais I. Mendgaziev[a], Vladimir A. Istomin[a,b], Daria V. Sergeeva[a,b], Vladimir A. Vinokurov[a], Yinghua Gong[a,c], Tianduo Li[c], Andrey S. Stoporev[a,d]

[a] *Gubkin University, Department of Physical and Colloid Chemistry, 65, Leninsky prospekt, Building 1, 119991 Moscow, Russian Federation*
[b] *Skolkovo Institute of Science and Technology (Skoltech), Nobelya Str. 3, 121205 Moscow, Russian Federation*
[c] *Shandong Provincial Key Laboratory of Molecular Engineering, School of Chemistry and Chemical Engineering, Qilu University of Technology (Shandong Academy of Sciences), Jinan 250353, PR China*
[d] *Department of Petroleum Engineering, Kazan Federal University, Kremlevskaya str. 18, Kazan 420008, Russian Federation*

A R T I C L E I N F O

Article history:
Received 17 October 2023
Revised 27 December 2023
Accepted 25 January 2024
Available online 9 February 2024

Dataset link: Raw data of gas hydrate equilibrium measurements for CH4 – MeOH – MgCl2 – H2O system and ice freezing point determination of aqueous MeOH and MgCl2 solutions (Original data)

Keywords:
Gas hydrates
Methane
Thermodynamic hydrate inhibitors
Phase equilibria
Methanol
Magnesium chloride
Ice freezing point

A B S T R A C T

In order to systematically study the synergistic effect of gas hydrate inhibition with mixtures of methanol (MeOH) and magnesium chloride ($MgCl_2$), the impact of these compounds on the thermodynamic stability of methane hydrate in the systems of CH_4–MeOH–H_2O, CH_4–$MgCl_2$–H_2O, and CH_4–MeOH–$MgCl_2$–H_2O was experimentally investigated. The pressure and temperature conditions of the three-phase vapor–aqueous solution–gas hydrate equilibrium were determined for these systems. The resulting dataset has 164 equilibrium points within the range of 234–289 K and 3–13 MPa. All equilibrium points were measured as the endpoint of methane hydrate dissociation during the heating stage. The phase boundaries of methane hydrate were identified for 8 systems with MeOH (up to 60 mass%), 5 $MgCl_2$ solutions (up to 26.7 mass%), and 14 mixtures of both inhibitors. Most equilibrium points were measured using a ramp heating technique (0.1 K/h) under isochoric conditions

DOI of original article: 10.1016/j.ces.2023.119361
* Corresponding author.
E-mail address: semenov.a@gubkin.ru (A.P. Semenov).

https://doi.org/10.1016/j.dib.2024.110138

when the fluids were stirred at 600 rpm. It was found that even a 0.5 K/h heating rate for the CH_4–$MgCl_2$–H_2O system at low salt concentrations, along with all mixed aqueous solutions with methanol, gives results that do not differ from 0.1 K/h, considering the measurement uncertainties. Most measurements for the CH_4–$MgCl_2$–H_2O system at high salt content were acquired using a step heating technique. The coefficients of the empirical equations approximating the equilibrium points for each inhibitor concentration were defined. The change in the slope parameter of the empirical equation was analyzed as a function of inhibitor content. Correlations that accurately describe the thermodynamic inhibition effect of methane hydrate with methanol and magnesium chloride on a mass% and mol% scale were obtained. The freezing temperatures of single and mixed aqueous solutions of methanol and magnesium chloride were determined experimentally to confirm the thermodynamic consistency of the methane hydrate equilibrium data.

Specifications Table

Subject	Chemistry
Specific subject area	Physical and Theoretical Chemistry
Type of data	Tables, figures
How the data were acquired	The pressure and temperature conditions of the three-phase coexistence of vapor–aqueous solution–gas hydrate were measured for systems containing water, gaseous methane, and methanol or magnesium chloride or their mixtures under intensive fluid agitation (600 rpm). All experiments were conducted under isochoric conditions. The ramp heating technique (0.1 K/h) was mainly used to measure the equilibrium points. Preliminary experiments at a higher heating rate of 0.5 K/h were performed for some solution samples. For concentrated magnesium chloride solutions, equilibrium conditions were determined using a step heating technique. The endpoint of methane hydrate dissociation was considered the equilibrium point. A GHA350 autoclave (PSL Systemtechnik, Germany) equipped with temperature and gauge pressure sensors, a stirrer, and a temperature control system was employed to conduct the experiments. The autoclave has the shape of a cylinder with a diameter of 0.085 m and a volume of 600 mL. A Hei-TORQUE 400 Precision overhead motor (Heidolph, Germany), a magnetic coupling (Premex, Switzerland), and a four-blade stirrer agitated the fluids. The blades have a height of 0.02 m and a diameter of 0.061 m. The blades are located at the lower end of the reactor at a distance of 0.005 m from the bottom. With a solution sample volume of 300 mL, the height of the liquid layer in the reactor is 0.06 m. At a rotational speed of 600 rpm, the Reynolds number for the tested solution samples is in the range of $9{\cdot}10^3$–$3.7{\cdot}10^4$ at 293.15 K (see Fig. 1 and description in section 2 in [1]). A liquid thermostat Ministat 240 or CC 505 (both Huber, Germany) filled with coolant (ethanol) circulating through the autoclave jacket controlled the temperature. Operation of the apparatus and recording of measured parameters during the experiment was automatic (PC with WinGHA software). The ice freezing point of the aqueous solution sample was measured in an 80 mL double-walled glass cell at 600 rpm. The sample temperature was logged by a calibrated PRT 5622–10-P quick-response probe combined with a 1524 reference thermometer (both Fluke, USA). Ethanol was circulated through the glass cell jacket using an F81-ME cryostat (Julabo, Germany). This allowed the sample temperature to change. The temperature at the plateau (or maximum) after the ice nucleation in the supercooled aqueous solution was assigned as the ice freezing point. Two consecutive measurements were made for each solution to achieve repeatability of ice freezing point $\leq$ 0.1 K.

(*continued on next page*)

Data format	Raw and analyzed
Description of data collection	The methane hydrate equilibrium data set contains 164 experimental points. For the CH_4–MeOH–H_2O system, 39 equilibrium points were measured for 8 different methanol concentrations in an aqueous solution: 5.00, 10.01, 20.00, 30.01, 39.99, 44.68, 49.99, and 60.00 mass%. For the CH_4–$MgCl_2$–H_2O system, 30 equilibrium points were measured for 5 different concentrations of magnesium chloride in an aqueous solution: 5.12, 8.43, 16.80, 22.28, and 26.68 mass%. For the CH_4–MeOH–$MgCl_2$–H_2O system containing both inhibitors, 83 equilibrium points were measured for 14 different mixed solutions with mass fractions of MeOH / $MgCl_2$: 5.00 / 5.13, 10.01 / 5.14, 19.99 / 5.13, 30.00 / 5.13, 40.00 / 4.80, 5.00 / 9.63, 10.00 / 9.62, 20.00 / 9.62, 30.00 / 9.61, 5.00 / 16.82, 10.00 / 16.82, 20.00 / 16.80, 5.00 / 21.60, 10.00 / 21.60 mass%. The dataset was supplemented with 12 equilibrium points for the CH_4–H_2O system without thermodynamic hydrate inhibitors (THI). The volume of an aqueous solution loaded into the autoclave was 300 mL, with the volume of the liquid phase equaling the residual autoclave space. The measured equilibrium points are in the 234–289 K and 3–13 MPa range of thermobaric parameters. Ice freezing points were measured at atmospheric pressure for 27 samples, including water, single and mixed aqueous methanol, and magnesium chloride solutions. The total number of freezing point measurements is 53. The ice freezing points determined are in the range of 217.60–273.15 K.
Data source location	Gubkin University, Department of Physical and Colloid Chemistry. Moscow, Russia. 55.692232°N, 37.55487°E
Data accessibility	Repository name: Mendeley Data Data identification number: 10.17632/ngr2pntbmy.1 Direct URL to data: https://data.mendeley.com/datasets/ngr2pntbmy/1
Related research article	A.P. Semenov, R.I. Mendgaziev, V.A. Istomin, D. V. Sergeeva, V.A. Vinokurov, Y. Gong, T. Li, A.S. Stoporev, Searching for synergy between alcohol and salt to produce more potent and environmentally benign gas hydrate inhibitors, Chem. Eng. Sci. 283 (2024) 119361. https://doi.org/10.1016/j.ces.2023.119361 [1].

1. Value of the data

- The data are useful for predicting the thermodynamic stability of methane hydrate over a wide range of inhibitor concentrations (methanol, magnesium chloride, and their mixtures), temperatures, and pressures.
- The data allows quantification of the synergistic effect of thermodynamic inhibition of methane hydrate with mixtures of methanol and magnesium chloride.
- The data provide a physicochemical basis for using mixed gas hydrate inhibitors based on methanol and magnesium chloride compositions that are more powerful and environmentally benign than single methanol.
- The data can be used to compare the thermodynamic inhibition of gas hydrates by methanol, magnesium chloride, and other compounds on a mass and mole fraction scale.
- Our data can be exploited to develop more accurate thermodynamic models and software to calculate the phase equilibria of gas hydrates in the presence of methanol, magnesium chloride, and their mixtures.

2. Objective

This dataset results from a systematic experimental study of the effects of methanol and magnesium chloride on methane hydrate equilibrium temperatures and pressures (coexisted vapor, aqueous solution, and gas hydrate phases). The experimental work was undertaken to gain new experimental data on the methane hydrate stability in the unexplored region of high magnesium chloride concentrations for the systems of CH_4–$MgCl_2$–H_2O and CH_4–MeOH–$MgCl_2$–H_2O [2] and to address the fundamental issue of how the concentration of alcohol and salt in an aqueous solution affects their synergistic effect in the thermodynamic inhibition of methane hydrate. The data obtained allowed us to derive precise correlations for quantitative analysis of the anti-hydrate activity of methanol and magnesium chloride in a wide range of concentrations (in mass and mole fraction scales) and pressures, based on which we determined how the

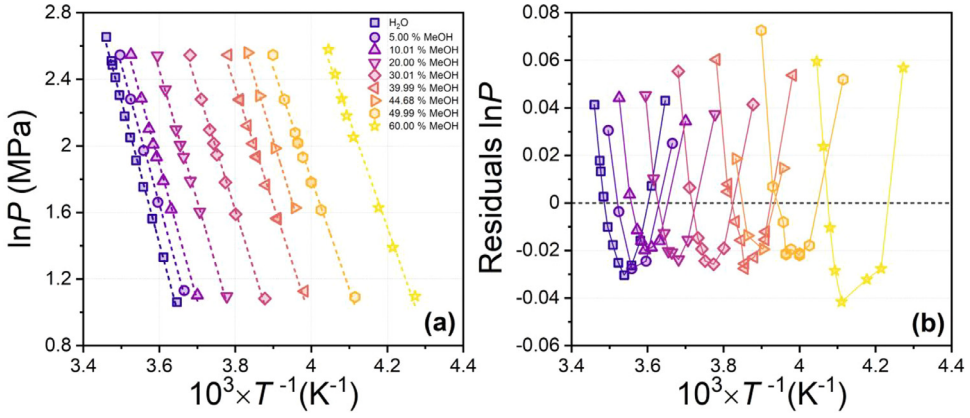

Fig. 1. **(a)** Measured methane hydrate equilibrium (V–L_w–H) points for a system of CH_4–MeOH–H_2O (together with our previous data from [7,8]) and approximations by two-parameter function $\ln P = A + B/T$ (color dashed lines, coefficients are in Table 2), the legend shows concentrations in mass%; **(b)** fitting residuals vs. independent variable of T^{-1}; the error bars are smaller than the symbol size.

synergism parameters depend on the composition of mixed gas hydrate inhibitors. The regularities that provide a better understanding of the mechanisms of thermodynamic inhibition of gas hydrates in systems containing two different types of inhibitors, including a polar organic compound (MeOH) and a salt electrolyte ($MgCl_2$), have also been established.

3. Data description

The raw data of the temperature and pressure measurements of the three-phase equilibrium (V–L_w–H) in the system of methane–methanol–magnesium chloride–water is collected in the archive "Gas hydrate equilibrium (CH_4-MeOH-$MgCl_2$-H_2O)" which is available via the link https://data.mendeley.com/datasets/ngr2pntbmy/1. The archive contains a single file for each measurement with columns for the following parameters: time (column A), temperature set-point (°C, column B), the temperature in the autoclave (°C, column C), the temperature of the coolant (°C, column D), gauge pressure (bar, column E), stirrer speed (rpm, column F), and stirrer torque (N·cm, column K). The file name specifies the equilibrium point number and the feed composition of the aqueous solution sample (in mass%). The original research paper presents examples of experimental pressure-temperature trajectories for ramp heating and step heating techniques (Figs. 2 and 3 in [1]). The equilibrium point coordinates were determined from the pressure-temperature curves obtained in each experiment. A summary of the experimental data, including system number, sample name, feed mass and mole fraction of MeOH and $MgCl_2$ in aqueous solution, point number, equilibrium temperature T and pressure P, methane hydrate equilibrium temperature suppression ΔT_h (relative to the pure water system), and measurement technique, is provided in Table 1. The comparison of the obtained equilibrium points with literature data for the systems of CH_4–MeOH–H_2O [3–8], CH_4–$MgCl_2$–H_2O [9–11], CH_4–MeOH–$MgCl_2$–H_2O [12] is available in the supported original paper [1].

Figs. 1–3 depict the results of approximating all obtained experimental points by the empirical equation $\ln P = A + B{\cdot}T^{-1}$. Panel b of Figs. 1–3 displays the fit residuals as a function of the independent variable (reciprocal T). Table 2 reports the numerical values of the fitting coefficients for each of the 28 aqueous phase samples. Fig. 4 demonstrates the variation of slope parameter B with the concentration of methanol and magnesium chloride for aqueous solutions containing a single inhibitor. The three-dimensional diagram in Fig. 5 illustrates the change of slope parameter B with the concentration of methanol and magnesium chloride, including for

Table 1
Measured methane hydrate equilibrium temperatures and pressures (V–L_w–H) with corresponding equilibrium temperature suppression values ΔT_h relative to pure water sample (H_2O).

# of system	Sample name	Feed mass fraction in aqueous solution		Feed mole fraction in aqueous solution		# of point	T / K[a]	P / MPa[b]	ΔT_h / K	Measurement technique
		ω_{MeOH}, mass%[c]	ω_{MgCl2}, mass%[c]	x_{MeOH}, mol%	x_{MgCl2}, mol%					
1	H_2O	0	0	0	0	1	274.25	2.891	0	0.1 K/h ramp heating
						2	276.96	3.785	0	0.1 K/h ramp heating
						3	279.26	4.771	0	0.1 K/h ramp heating
						4	281.11	5.777	0	0.1 K/h ramp heating
						5	282.62	6.77	0	0.1 K/h ramp heating
						6	283.87	7.776	0	0.1 K/h ramp heating
						7	285.01	8.839	0	0.1 K/h ramp heating
						8	286.14	10.027	0	0.1 K/h ramp heating
						9	287.03	11.143	0	0.1 K/h ramp heating
						10	287.65	12.009	0	0.1 K/h ramp heating
						11	287.85	12.316	0	0.1 K/h ramp heating
						12	289.02	14.222	0	0.1 K/h ramp heating
2	5Me	5.00	0	2.87	0	13	272.83	3.10	2.12	0.1 K/h ramp heating
						14	278.10	5.27	2.12	0.1 K/h ramp heating
						15	281.04	7.19	2.14	0.1 K/h ramp heating
						16	283.76	9.79	2.15	0.1 K/h ramp heating
						17	286.01	12.77	2.14	0.1 K/h ramp heating
3	10Me	10.01	0	5.89	0	18	270.26	3.01	4.41	0.1 K/h ramp heating
						19	275.40	5.05	4.42	0.1 K/h ramp heating
						20	281.50	9.82	4.46	0.1 K/h ramp heating
						21	283.68	12.79	4.48	0.1 K/h ramp heating
4	20Me	20.00	0	12.32	0	22	264.73	2.99	9.86	0.1 K/h ramp heating
						23	269.83	4.98	9.84	0.1 K/h ramp heating
						24	276.55	10.37	9.88	0.1 K/h ramp heating
						25	278.19	12.71	9.91	0.1 K/h ramp heating

(*continued on next page*)

Table 1 (*continued*)

# of system	Sample name	Feed mass fraction in aqueous solution		Feed mole fraction in aqueous solution		# of point	T / K[a]	P / MPa[b]	ΔT_h / K	Measurement technique
		ω_{MeOH}, mass%[c]	ω_{MgCl2}, mass%[c]	x_{MeOH}, mol%	x_{MgCl2}, mol%					
5	30Me	30.01	0	19.42	0	26	257.88	2.95	16.58	0.1 K/h ramp heating
						27	263.12	4.90	16.41	0.1 K/h ramp heating
						28	269.53	9.78	16.38	0.1 K/h ramp heating
						29	271.69	12.75	16.45	0.1 K/h ramp heating
6	40Me	39.99	0	27.26	0	30	251.13	3.09	23.77	0.1 K/h ramp heating
						31	255.69	4.76	23.54	0.1 K/h ramp heating
						32	255.76	4.78	23.53	0.1 K/h ramp heating
						33	262.32	9.73	23.55	0.1 K/h ramp heating
						34	262.39	9.77	23.55	0.1 K/h ramp heating
						35	264.48	12.76	23.66	0.1 K/h ramp heating
7	44.7Me	44.68	0	31.23	0	36	252.75	5.09	27.14	0.1 K/h ramp heating
						37	256.15	7.29	27.15	0.1 K/h ramp heating
						38	258.89	9.98	27.18	0.1 K/h ramp heating
						39	260.95	12.94	27.31	0.1 K/h ramp heating
8	50Me	49.99	0	35.99	0	40	243.02	2.98	31.53	0.1 K/h ramp heating
						41	248.42	5.03	31.38	0.1 K/h ramp heating
						42	254.50	9.76	31.43	0.1 K/h ramp heating
						43	256.49	12.76	31.64	0.1 K/h ramp heating
9	60Me	60.00	0	45.75	0	44	234.03	2.99	40.53	stepwise heating
						45	237.27	4.01	40.39	stepwise heating
						46	239.40	5.10	40.39	stepwise heating
						47	243.28	7.78	40.61	0.1 K/h ramp heating
						48	244.34	8.85	40.73	0.1 K/h ramp heating
						49	245.12	9.81	40.83	0.1 K/h ramp heating
						50	246.17	11.36	40.99	0.1 K/h ramp heating
						51	247.23	13.18	41.18	0.1 K/h ramp heating

(*continued on next page*)

Table 1 (*continued*)

# of system	Sample name	Feed mass fraction in aqueous solution		Feed mole fraction in aqueous solution		# of point	T / K[a]	P / MPa[b]	ΔT_h / K	Measurement technique
		ω_{MeOH}, mass%[c]	ω_{MgCl2}, mass%[c]	x_{MeOH}, mol%	x_{MgCl2}, mol%					
10	5.1Mg	0	5.12	0	1.01	52	272.72	3.07	2.14	0.1 K/h ramp heating
						53	277.85	5.16	2.16	0.1 K/h ramp heating
						54	281.12	7.29	2.19	0.1 K/h ramp heating
						55	283.73	9.81	2.20	0.1 K/h ramp heating
						56	285.99	12.80	2.18	0.1 K/h ramp heating
11	8.4Mg	0	8.43	0	1.71	57	271.06	3.12	3.94	**0.5 K/h** ramp heating
						58	271.08	3.15	4.03	0.1 K/h ramp heating
						59	275.95	5.15	4.06	0.1 K/h ramp heating
						60	279.20	7.33	4.13	0.1 K/h ramp heating
						61	281.72	9.77	4.19	0.1 K/h ramp heating
						62	283.81	12.58	4.21	0.1 K/h ramp heating
12	16.8Mg	0	16.80	0	3.68	63	262.54	3.17	12.65	0.1 K/h ramp heating
						64	267.22	5.16	12.80	0.1 K/h ramp heating
						65	270.38	7.33	12.98	0.1 K/h ramp heating
						66	272.78	9.82	13.15	0.1 K/h ramp heating
						67	274.80	12.68	13.30	0.1 K/h ramp heating
13	22.3Mg	0	22.28	0	5.15	68	251.43	3.04	23.33	stepwise heating
						69	256.37	5.16	23.65	stepwise heating
						70	256.45	5.17	23.58	0.1 K/h ramp heating
						71	259.38	7.26	23.89	stepwise heating
						72	261.67	9.72	24.17	stepwise heating
						73	263.57	12.44	24.37	0.1 K/h ramp heating
						74	263.75	12.99	24.54	stepwise heating
14	26.7Mg	0	26.68	0	6.44	75	238.98	3.17[d]	36.19[d]	stepwise heating
						76	243.23	5.11[d]	36.66[d]	stepwise heating
						77	245.66	6.86[d]	37.15[d]	stepwise heating
						78	248.06	9.75[d]	37.77[d]	stepwise heating
						79	248.39	9.76[d]	37.50[d]	0.1 K/h ramp heating
						80	250.02	12.91[d]	38.21[d]	stepwise heating
						81	250.12	13.06[d]	38.23[d]	stepwise heating

(*continued on next page*)

Table 1 (*continued*)

# of system	Sample name	Feed mass fraction in aqueous solution		Feed mole fraction in aqueous solution		# of point	T / K[a]	P / MPa[b]	ΔT_h / K	Measurement technique
		ω_{MeOH}, mass%[c]	ω_{MgCl2}, mass%[c]	x_{MeOH}, mol%	x_{MgCl2}, mol%					
15	5Me5.1Mg	5.00	5.13	3.00	1.04	82	270.46	3.13	4.58	0.1 K/h ramp heating
						83	275.30	5.13	4.67	0.1 K/h ramp heating
						84	278.67	7.33	4.67	0.1 K/h ramp heating
						85	281.22	9.82	4.72	0.1 K/h ramp heating
						86	283.41	12.80	4.77	0.1 K/h ramp heating
16	10Me5.1Mg	10.01	5.14	6.15	1.06	87	267.56	3.09	7.35	0.1 K/h ramp heating
						88	268.58	3.42	7.37	0.1 K/h ramp heating
						89	272.25	4.97	7.42	0.1 K/h ramp heating
						90	274.40	6.26	7.47	0.1 K/h ramp heating
						91	277.88	9.22	7.52	0.1 K/h ramp heating
						92	280.65	12.90	7.59	0.1 K/h ramp heating
17	20Me5.1Mg	19.99	5.13	12.90	1.11	93	261.46	3.21	13.83	0.1 K/h ramp heating
						94	262.28	3.49	13.87	0.1 K/h ramp heating
						95	265.97	5.06	13.86	0.1 K/h ramp heating
						96	268.22	6.31	13.73	0.1 K/h ramp heating
						97	271.69	9.25	13.74	0.1 K/h ramp heating
						98	274.04	12.76	14.11	0.1 K/h ramp heating
18	30Me5.1Mg	30.00	5.13	20.40	1.17	99	253.53	3.16	21.61	0.1 K/h ramp heating
						100	253.59	3.17	21.59	**0.5 K/h** ramp heating
						101	258.48	5.18	21.59	0.1 K/h ramp heating
						102	261.76	7.34	21.59	0.1 K/h ramp heating
						103	264.32	9.91	21.70	0.1 K/h ramp heating
						104	266.27	12.69	21.84	0.1 K/h ramp heating
19	40Me4.8Mg	40.00	4.80	28.61	1.16	105	246.75	3.56	29.61	0.1 K/h ramp heating
						106	250.41	5.14	29.57	0.1 K/h ramp heating
						107	250.49	5.17	29.55	**0.5 K/h** ramp heating
						108	253.61	7.31	29.70	0.1 K/h ramp heating
						109	256.05	9.81	29.89	0.1 K/h ramp heating
						110	258.04	12.77	30.12	0.1 K/h ramp heating
20	5Me9.6Mg	5.00	9.63	3.12	2.02	111	267.25	3.14	7.82	0.1 K/h ramp heating
						112	272.05	5.12	7.89	0.1 K/h ramp heating
						113	275.46	7.40	7.97	0.1 K/h ramp heating
						114	277.74	9.69	8.09	0.1 K/h ramp heating
						115	280.02	12.86	8.19	0.1 K/h ramp heating

(*continued on next page*)

Table 1 (*continued*)

# of system	Sample name	Feed mass fraction in aqueous solution		Feed mole fraction in aqueous solution		# of point	T / K[a]	P / MPa[b]	ΔT_h / K	Measurement technique
		ω_{MeOH}, mass%[c]	ω_{MgCl2}, mass%[c]	x_{MeOH}, mol%	x_{MgCl2}, mol%					
21	10Me9.6Mg	10.00	9.62	6.40	2.07	116	264.47	3.25	10.96	0.1 K/h ramp heating
						117	264.52	3.26	10.93	**0.5 K/h** ramp heating
						118	268.92	5.16	11.10	0.1 K/h ramp heating
						119	272.30	7.43	11.17	0.1 K/h ramp heating
						120	274.60	9.76	11.30	0.1 K/h ramp heating
						121	276.82	12.88	11.41	0.1 K/h ramp heating
22	20Me9.6Mg	20.00	9.62	13.47	2.18	122	256.64	3.20	18.64	0.1 K/h ramp heating
						123	256.69	3.21	18.60	**0.5 K/h** ramp heating
						124	261.26	5.16	18.77	0.1 K/h ramp heating
						125	264.52	7.43	18.95	0.1 K/h ramp heating
						126	266.87	9.83	19.08	0.1 K/h ramp heating
						127	268.99	12.94	19.27	0.1 K/h ramp heating
23	30Me9.6Mg	30.00	9.61	21.33	2.30	128	247.53	3.16	27.62	0.1 K/h ramp heating
						129	252.10	5.03	27.68	**0.5 K/h** ramp heating
						130	252.11	5.03	27.66	0.1 K/h ramp heating
						131	255.49	7.35	27.88	0.1 K/h ramp heating
						132	257.81	9.75	28.07	0.1 K/h ramp heating
						133	259.90	12.89	28.33	0.1 K/h ramp heating
24	5Me16.8Mg	5.00	16.82	3.34	3.78	134	259.06	3.32	16.57	**0.5 K/h** ramp heating
						135	259.06	3.31	16.56	0.1 K/h ramp heating
						136	263.16	5.13	16.81	0.1 K/h ramp heating
						137	266.42	7.39	16.99	0.1 K/h ramp heating
						138	268.82	9.81	17.12	0.1 K/h ramp heating
						139	270.76	12.83	17.43	0.1 K/h ramp heating

(*continued on next page*)

Table 1 (*continued*)

# of system	Sample name	Feed mass fraction in aqueous solution		Feed mole fraction in aqueous solution		# of point	T / K[a]	P / MPa[b]	ΔT_h / K	Measurement technique
		ω_{MeOH}, mass%[c]	ω_{MgCl2}, mass%[c]	x_{MeOH}, mol%	x_{MgCl2}, mol%					
25	10Me16.8Mg	10.00	16.82	6.86	3.88	140	254.23	3.12	20.80	**0.5 K/h** ramp heating
						141	254.16	3.13	20.89	0.1 K/h ramp heating
						142	258.81	5.10	21.10	0.1 K/h ramp heating
						143	261.88	7.26	21.37	0.1 K/h ramp heating
						144	261.88	7.26	21.38	0.1 K/h ramp heating
						145	264.12	9.57	21.61	0.1 K/h ramp heating
						146	266.31	12.92	21.94	0.1 K/h ramp heating
26	20Me16.8Mg	20.00	16.80	14.49	4.10	147	244.38	3.17	30.78	0.1 K/h ramp heating
						148	248.65	4.97	31.01	**0.5 K/h** ramp heating
						149	248.56	4.95	31.06	0.1 K/h ramp heating
						150	251.47	6.96	31.39	0.1 K/h ramp heating
						151	253.90	9.43	31.70	0.1 K/h ramp heating
						152	256.08	12.92	32.17	0.1 K/h ramp heating
27	5Me21.6Mg	5.00	21.60	3.50	5.09	153	249.08	3.25	26.36	0.1 K/h ramp heating
						154	249.08	3.26	26.39	**0.5 K/h** ramp heating
						155	253.49	5.25	26.70	0.1 K/h ramp heating
						156	256.51	7.41	26.93	0.1 K/h ramp heating
						157	258.60	9.77	27.30	0.1 K/h ramp heating
						158	260.47	12.83	27.73	0.1 K/h ramp heating
28	10Me21.6Mg	10.00	21.60	7.20	5.23	159	244.45	3.49	31.71	0.1 K/h ramp heating
						160	247.95	5.13	32.02	**0.5 K/h** ramp heating
						161	247.85	5.13	32.11	0.1 K/h ramp heating
						162	250.51	7.07	32.50	0.1 K/h ramp heating
						163	252.86	9.55	32.85	0.1 K/h ramp heating
						164	254.87	12.77	33.29	0.1 K/h ramp heating

[a] Expanded uncertainty of temperature measurements is 0.1 K ($k = 2$).
[b] Expanded uncertainty of pressure measurements is 0.02 MPa ($k = 2$).
[c] Expanded uncertainties ($k = 2$) of the methanol and magnesium chloride mass fractions are given in the original research paper [1] (see Table 1).
[d] Metastable equilibrium vapor – supercooled aqueous solution – gas hydrate (an aqueous solution of magnesium chloride is supercooled relative to the crystalline hydrate phase $MgCl_2 \cdot 12H_2O$). See Section 3.1 of the original research paper [1] for a more detailed discussion.

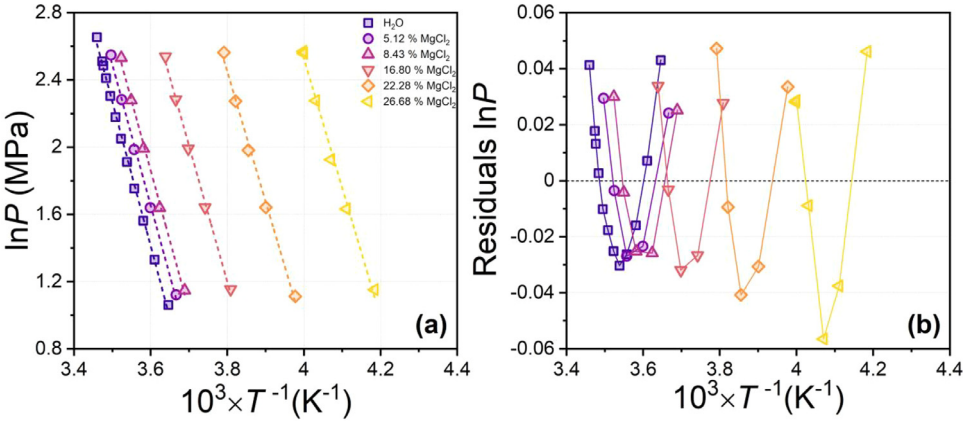

Fig. 2. **(a)** Measured methane hydrate equilibrium (V–L_w–H) points for a system of CH_4–$MgCl_2$–H_2O and approximations by two-parameter function $\ln P = A + B/T$ (color dashed lines, coefficients are in Table 2), the legend shows concentrations in mass%; **(b)** fitting residuals vs. independent variable of T^{-1}; the error bars are smaller than the symbol size.

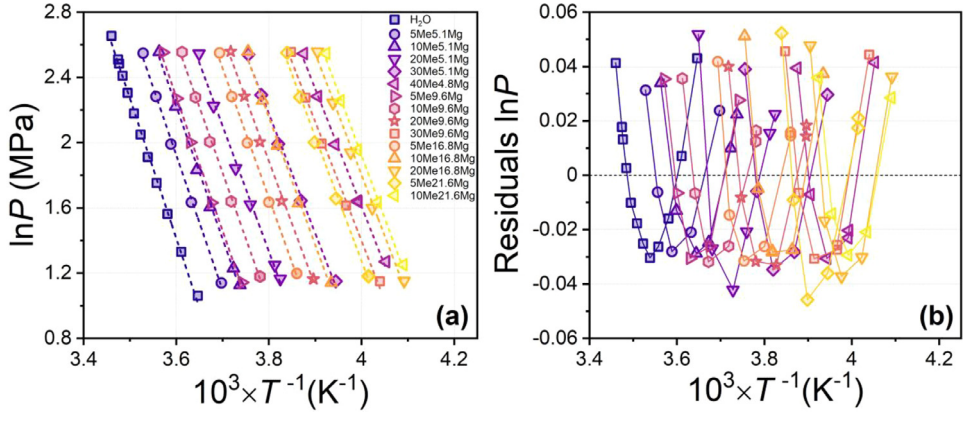

Fig. 3. **(a)** Measured methane hydrate equilibrium (V–L_w–H) points for the mixed system of CH_4–MeOH–$MgCl_2$–H_2O and approximations by two-parameter function $\ln P = A + B/T$ (color dashed lines, coefficients are in Table 2), the first number in the designation of the mixed sample is the concentration of MeOH, the second number is the concentration of $MgCl_2$ in mass%; **(b)** fitting residuals vs. independent variable of T^{-1}; the error bars are smaller than the symbol size.

mixed inhibitors. The numerical values of the approximation parameters for another empirical function $\ln P = A + B{\cdot}T^{-1} + C{\cdot}\ln T$ are in Table 3. Figs. 6–8 show graphically the approximation data of the experimental points by the given equation with three coefficients.

The previously proposed correlation [13] was applied to describe the thermodynamic inhibition effect of methane hydrate (ΔT_h) by methanol and magnesium chloride in two concentration scales (mass% and mol%). The numerical values of the coefficients for the systems CH_4–MeOH–H_2O and CH_4–$MgCl_2$–H_2O are listed in Tables 4 and 5, respectively. The experimental and calculated ΔT_h and the difference between them for the system of CH_4–MeOH–H_2O are in Tables 6 and 7. Similar numerical data for the CH_4–$MgCl_2$–H_2O system are in Tables 8 and 9.

Methane hydrate equilibrium temperature suppression ΔT_h is plotted against equilibrium pressure for aqueous solutions of methanol (Fig. 9) and magnesium chloride (Fig. 10). The color

Table 2
Parameters of approximation by empirical function ln $P = A + B/T$ of methane hydrate equilibrium points in the pressure range of 3–13 MPa for systems of CH_4–H_2O (data from [13]), CH_4–MeOH–H_2O (concatenated dataset of this work and from [7,8]), CH_4–$MgCl_2$–H_2O (data of this work), CH_4–MeOH–$MgCl_2$–H_2O (data of this work).

#	Aqueous solution sample	A		B, K		Adjusted R^2
		Value	Standard Error	Value	Standard Error	
1	H_2O	32.23	0.48	−8559.31	135.56	0.99725
2	5Me	31.71	0.85	−8349.32	237.14	0.99678
3	10Me	31.42	0.70	−8202.36	194.70	0.99607
4	20Me	30.79	0.73	−7870.90	199.40	0.99552
5	30Me	29.56	0.80	−7353.29	214.02	0.99410
6	40Me	29.06	0.69	−7029.24	178.12	0.99362
7	44.7Me[a]	31.16[a]	0.99[a]	−7467.30[a]	254.51[a]	0.99652
8	50Me	28.36	0.82	−6638.46	206.48	0.99136
9	60Me	28.77	0.85	−6490.17	206.80	0.99294
10	5.1Mg	31.75	0.81	−8358.36	226.27	0.99708
11	8.4Mg	31.88	0.85	−8337.02	236.59	0.99679
12	16.8Mg	32.04	0.97	−8117.03	260.61	0.99589
13	22.3Mg	31.86	1.19	−7739.53	308.58	0.99367
14	26.7Mg[b]	33.33	1.15	−7699.98	282.68	0.99330
15	5Me5.1Mg	31.80	0.83	−8298.34	229.96	0.99694
16	10Me5.1Mg	31.51	0.69	−8134.74	189.22	0.99730
17	20Me5.1Mg	30.60	0.95	−7703.20	253.81	0.99460
18	30Me5.1Mg	29.99	0.99	−7320.10	257.82	0.99506
19	40Me4.8Mg	30.45	0.98	−7209.30	248.24	0.99410
20	5Me9.6Mg	31.89	0.95	−8223.82	261.14	0.99598
21	10Me9.6Mg	31.60	0.68	−8050.93	184.31	0.99739
22	20Me9.6Mg	31.10	0.74	−7687.73	194.34	0.99681
23	30Me9.6Mg	30.62	1.01	−7306.45	257.85	0.99380
24	5Me16.8Mg	31.88	0.77	−7953.57	202.46	0.99677
25	10Me16.8Mg	31.87	1.08	−7818.72	283.00	0.99348
26	20Me16.8Mg	31.66	1.23	−7463.56	309.12	0.99317
27	5Me21.6Mg	31.76	0.98	−7620.23	250.30	0.99463
28	10Me21.6Mg	32.75	1.05	−7706.71	262.76	0.99537

[a] Experimental points for the 44.7Me sample are available for a narrower pressure range of 5–13 MPa, so the values of the approximation parameters for it are clearly out of line with other samples in the CH_4–MeOH–H_2O system.

[b] Metastable equilibrium vapor – supercooled aqueous solution – gas hydrate (an aqueous solution of magnesium chloride is supercooled relative to the crystalline hydrate phase $MgCl_2 \cdot 12H_2O$). See Section 3.1 of the original research paper [1] for a more detailed discussion.

contour plots in Fig. 11 provide a complete overview of the methanol inhibition activity in the mass% and mol% scales. The similar contour plots for aqueous solutions of magnesium chloride are in Fig. 12. Fig. 13 shows the magnitude of ΔT_h as a function of equilibrium pressure for mixed MeOH+$MgCl_2$ inhibitors.

Figs. 14 and 15 display experimental pressure and temperature curves for the 10Me16.8Mg and 26.7Mg aqueous solution samples, respectively. The curves were obtained by measuring the three-phase equilibrium gas–aqueous solution–gas hydrate using ramp heating technique (0.1 K/h) for the former and step heating technique for the latter.

The unprocessed data from the ice-freezing temperature measurements of aqueous methanol and magnesium chloride solutions at ambient pressure can be found in the "Ice freezing points (MeOH-$MgCl_2$-H_2O)" archive. There are files for 53 experiments. The file name denotes the number of the measurement and the concentration of the solute in the aqueous solution (methanol or magnesium chloride or a mixture of them) in mass%. Each file contains columns with the recorded sample temperatures and the time from the start of the measurement. Table 10 summarizes numerical data on ice freezing temperatures for the studied samples. A comparison of the obtained ice freezing temperatures with the data of other authors for the

Table 3
Parameters of approximation by empirical function $\ln P = A + B/T + C \cdot \ln T$ of methane hydrate equilibrium points in the pressure range of 3–13 MPa for systems of CH_4–H_2O (data from [13]), CH_4–MeOH–H_2O (concatenated dataset of this work and from [7,8]), CH_4–$MgCl_2$–H_2O (data of this work), CH_4–MeOH–$MgCl_2$–H_2O (data of this work).

#	Aqueous solution sample	*A*		*B*, K		*C*		Adjusted R^2
		Value	Standard Error	Value	Standard Error	Value	Standard Error	
1	H_2O	−1326.82	65.07	49,110.55	2761.27	204.63	9.80	0.99994
2	5Me	−1321.98	78.78	48,641.13	3316.82	204.11	11.88	0.99997
3	10Me	−1322.00	73.47	48,347.42	3070.03	204.35	11.09	0.99993
4	20Me	−1356.55	79.14	49,128.64	3251.44	210.10	11.98	0.99991
5	30Me	−1435.62	87.11	51,563.92	3503.02	222.74	13.24	0.99988
6	40Me	−1558.91	90.49	55,445.42	3560.35	242.36	13.81	0.99982
7	44.7Me[a]	−1937.09[a]	178.03[a]	69,703.24[a]	6980.09[a]	300.58[a]	27.19[a]	0.99994
8	50Me	−1509.26	130.43	52,208.58	4992.08	235.84	20.01	0.99953
9	60Me	−1833.34	181.65	62,622.35	6742.21	287.21	28.02	0.99961
10	5.1Mg	−1270.80	82.33	46,468.36	3465.64	196.41	12.41	0.99997
11	8.4Mg	−1403.90	53.24	51,750.20	2228.09	216.72	8.04	0.99999
12	16.8Mg	−1597.86	120.80	58,259.09	4919.50	247.22	18.32	0.99993
13	22.3Mg	−1832.37	247.43	65,506.18	9721.71	284.59	37.77	0.99968
14	26.7Mg[b]	−2155.08	206.44	74,686.22	7771.96	336.67	31.76	0.99977
15	5Me5.1Mg	−1327.52	147.75	48,499.95	6173.86	205.23	22.31	0.99989
16	10Me5.1Mg	−1316.52	90.26	47,684.15	3737.67	203.86	13.65	0.99995
17	20Me5.1Mg	−1762.03	412.59	65,061.37	16,747.73	272.06	62.62	0.99901
18	30Me5.1Mg	−1513.15	168.61	53,776.73	6675.86	235.24	25.70	0.99983
19	40Me4.8Mg	−1858.56	87.76	65,800.10	3391.90	289.23	13.44	0.99995
20	5Me9.6Mg	−1538.48	119.33	56,723.87	4935.25	237.53	18.05	0.99993
21	10Me9.6Mg	−1452.23	134.64	52,684.64	5511.04	224.86	20.40	0.99992
22	20Me9.6Mg	−1536.07	108.41	54,877.34	4327.87	238.55	16.50	0.99994
23	30Me9.6Mg	−1694.05	107.85	59,636.48	4186.30	263.86	16.50	0.99990
24	5Me16.8Mg	−1655.98	263.96	59,897.57	10,611.14	256.60	40.13	0.99971
25	10Me16.8Mg	−1849.37	115.84	66,726.19	4590.15	286.74	17.66	0.99990
26	20Me16.8Mg	−1927.06	227.30	67,640.12	8715.75	300.33	34.85	0.99973
27	5Me21.6Mg	−2128.57	275.02	76,387.87	10,694.70	330.40	42.06	0.99967
28	10Me21.6Mg	−1856.70	214.32	64,614.73	8203.53	289.80	32.87	0.99983

[a] Experimental points for the 44.7Me sample are available for a narrower pressure range of 5–13 MPa, so the values of the approximation parameters for it are clearly out of line with other samples in the CH_4–MeOH–H_2O system.

[b] Metastable equilibrium vapor – supercooled aqueous solution – gas hydrate (an aqueous solution of magnesium chloride is supercooled relative to the crystalline hydrate phase $MgCl_2 \cdot 12H_2O$). See Section 3.1 of the original research paper [1] for a more detailed discussion.

Table 4
Parameters of surface fitting by empirical function 4 from ref. [13] of methane hydrate equilibrium temperature suppression ΔT_h vs. methanol content in water solution (0–60 mass% or 0–45.75 mol%) and pressure (3–13 MPa); (concatenated dataset of this work and from ref. [7,8] for CH_4–MeOH–H_2O system).

Coefficient	mass% scale	mol% scale
b_1	1473.0833357	1641.7054402
b_2	33.3833535	37.1738314
b_3	−0.4185953	−0.9965618
b_4	0.0034765	0.0095137
b_5	$2.5055388 \cdot 10^{-4}$	$4.1235123 \cdot 10^{-4}$
b_6	$-7.5099827 \cdot 10^{-7}$	$-1.1868746 \cdot 10^{-6}$
b_7	$6.3389845 \cdot 10^{-8}$	$1.0082277 \cdot 10^{-7}$
Adjusted R^2	0.99996	0.99997
Average absolute deviation (K)	0.08	0.06
Average absolute relative deviation (%)	0.80	0.64

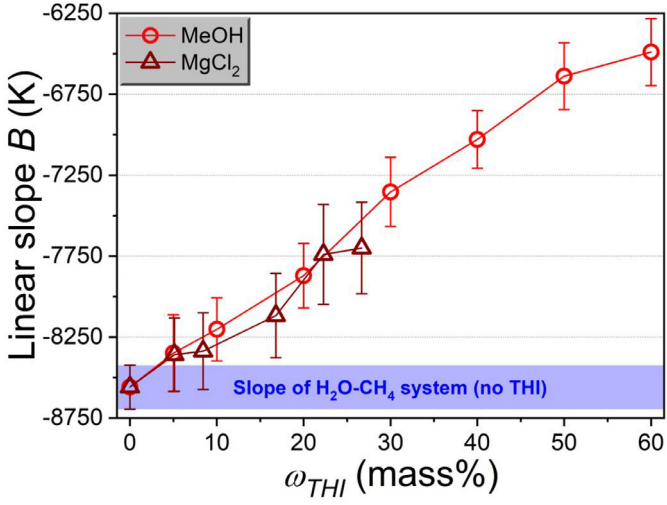

Fig. 4. Parameter B (empirical equation $\ln P = A + B/T$) vs. concentration of MeOH or $MgCl_2$ in system CH_4–THI–H_2O; symbols and error bars are values and standard errors of linear slope B (collected in Table 2); blue area displays B value and standard error for the uninhibited system of CH_4–H_2O.

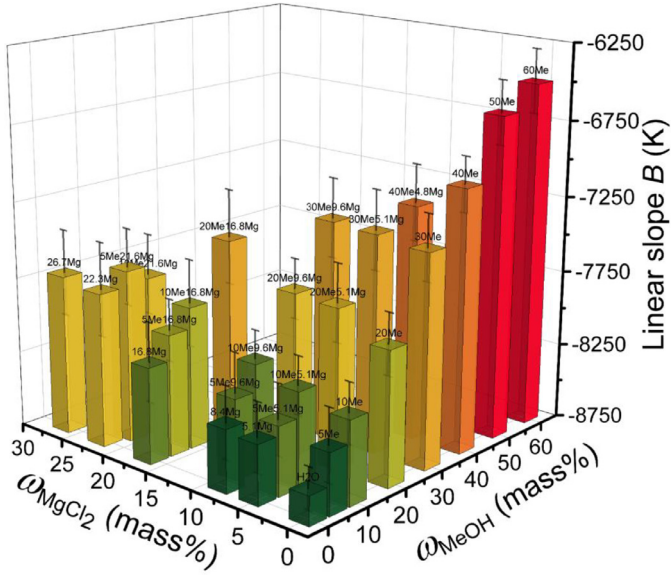

Fig. 5. Parameter B (empirical equation $\ln P = A + B/T$) vs. concentration of THIs in the mixed system of CH_4–MeOH–$MgCl_2$–H_2O; error bars are standard errors of linear slope B (see Table 2).

systems of $MgCl_2$–H_2O [14] and MeOH–H_2O [15,16] is available in the original paper (Fig. 14 in ref. [1]).

The data in Table 11 exemplify the approach of Hu et al. [17] to test our methane hydrate equilibrium data for thermodynamic consistency. A more detailed discussion is available in the Section 3.5 of the original research paper [1].

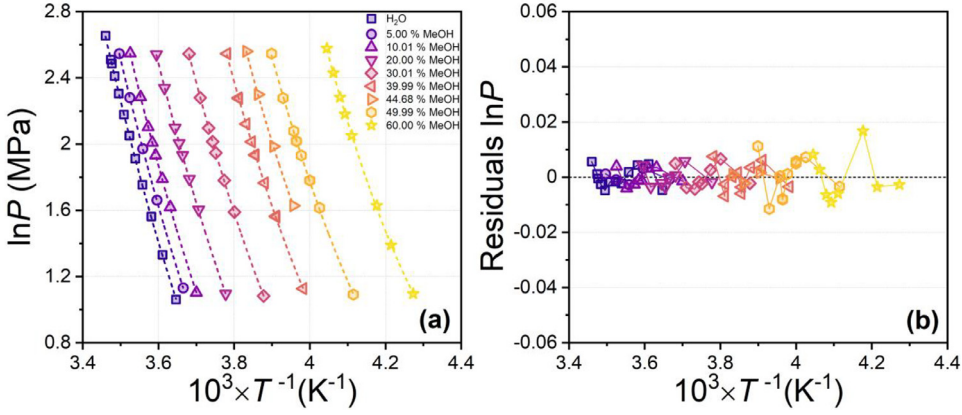

Fig. 6. **(a)** Measured methane hydrate equilibrium (V–L_w–H) points for a system of CH_4–MeOH–H_2O (together with our previous data from [7,8]) and approximations by three-parameter function $\ln P = A + B/T + C\cdot\ln T$ (color dashed lines, coefficients are in Table 3), the legend shows concentrations in mass%; **(b)** fitting residuals vs. independent variable of T^{-1}; the error bars are smaller than the symbol size.

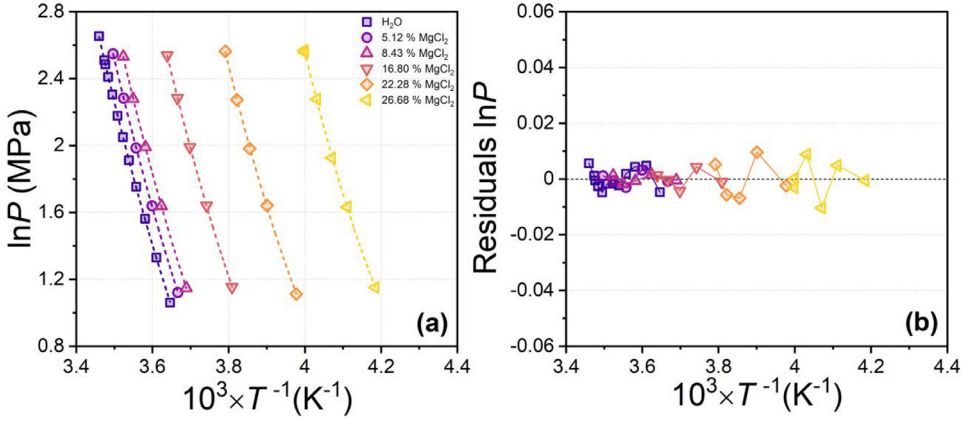

Fig. 7. **(a)** Measured methane hydrate equilibrium (V–L_w–H) points for a system of CH_4–$MgCl_2$–H_2O and approximations by three-parameter function $\ln P = A + B/T + C\cdot\ln T$ (color dashed lines, coefficients are in Table 3), the legend shows concentrations in mass%; **(b)** fitting residuals vs. independent variable of T^{-1}; the error bars are smaller than the symbol size.

Table 5
Parameters of surface fitting by empirical function 4 from ref. [13] of methane hydrate equilibrium temperature suppression ΔT_h vs. $MgCl_2$ content in water solution (0–26.68 mass% or 0–6.44 mol%) and pressure (3–13 MPa); (data of this work for CH_4–$MgCl_2$–H_2O system).

Coefficient	mass% scale	mol% scale
b_1	226.0459951	12.0159758
b_2	5.2057634	0.788412
b_3	0.4108187	0.6164673
b_4	0.011339	−0.0245248
b_5	0.0015167	0.1517817
b_6	$1.3402534\cdot10^{-5}$	0.0013412
b_7	$-2.9001212\cdot10^{-7}$	$-2.9022466\cdot10^{-5}$
Adjusted R^2	0.999996	0.999996
Average absolute deviation (K)	0.02	0.02
Average absolute relative deviation (%)	0.31	0.31

Table 6
Results of surface fitting by empirical function 4 from ref. [13] of methane hydrate equilibrium temperature suppression ΔT_h vs. MeOH content in water solution in mass% scale and gas pressure for CH_4–MeOH–H_2O system (concatenated dataset of this work and from ref. [7,8]).

MeOH mass fraction, mass%	*P*, MPa	ΔT_h experiment, K	ΔT_h fit, K	Residuals of ΔT_h (experiment–fit), K
0	2.89	0	0	0
0	3.79	0	0	0
0	4.77	0	0	0
0	5.78	0	0	0
0	6.77	0	0	0
0	7.78	0	0	0
0	8.84	0	0	0
0	10.03	0	0	0
0	11.14	0	0	0
0	12.01	0	0	0
0	12.32	0	0	0
0	13.20	0	0	0
5.00	3.10	2.12	2.03	0.09
5.00	5.27	2.12	2.02	0.09
5.00	7.19	2.14	2.02	0.11
5.00	9.79	2.15	2.03	0.12
5.00	12.77	2.14	2.05	0.09
10.01	3.01	4.41	4.41	−0.00
10.01	5.05	4.42	4.40	0.03
10.01	5.99	4.43	4.40	0.03
10.01	6.90	4.44	4.40	0.04
10.01	7.45	4.44	4.40	0.04
10.01	8.19	4.44	4.40	0.04
10.01	9.82	4.46	4.41	0.04
10.01	12.79	4.48	4.45	0.03
20.00	2.99	9.86	9.96	−0.10
20.00	4.98	9.84	9.94	−0.10
20.00	5.99	9.84	9.94	−0.10
20.00	6.91	9.84	9.94	−0.10
20.00	7.43	9.84	9.94	−0.10
20.00	8.15	9.85	9.95	−0.10
20.00	10.37	9.88	9.99	−0.11
20.00	12.71	9.91	10.06	−0.14
30.01	2.95	16.58	16.37	0.21
30.01	4.90	16.41	16.34	0.07
30.01	5.94	16.37	16.33	0.04
30.01	7.01	16.36	16.34	0.02
30.01	7.50	16.36	16.35	0.01
30.01	8.14	16.36	16.36	0.01
30.01	9.78	16.38	16.40	−0.02
30.01	12.75	16.45	16.53	−0.08
39.99	3.09	23.77	23.49	0.28
39.99	4.76	23.54	23.45	0.08
39.99	4.78	23.53	23.45	0.08
39.99	5.84	23.49	23.45	0.05
39.99	6.91	23.49	23.45	0.03
39.99	6.93	23.49	23.45	0.03
39.99	7.49	23.49	23.46	0.03
39.99	8.35	23.51	23.48	0.03
39.99	9.73	23.55	23.53	0.01
39.99	9.77	23.55	23.53	0.01
39.99	12.76	23.66	23.73	−0.07
44.67	5.09	27.14	27.06	0.08
44.67	7.29	27.15	27.07	0.08
44.67	9.98	27.18	27.17	0.01
44.67	12.94	27.31	27.40	−0.09

(*continued on next page*)

Table 6 (*continued*)

MeOH mass fraction, mass%	*P*, MPa	ΔT_h experiment, K	ΔT_h fit, K	Residuals of ΔT_h (experiment–fit), K
49.99	2.98	31.53	31.48	0.05
49.99	5.03	31.38	31.42	−0.03
49.99	5.93	31.36	31.41	−0.05
49.99	5.94	31.36	31.41	−0.05
49.99	6.90	31.35	31.42	−0.07
49.99	7.52	31.35	31.43	−0.08
49.99	7.53	31.35	31.43	−0.08
49.99	7.99	31.36	31.44	−0.08
49.99	9.76	31.43	31.53	−0.09
49.99	12.76	31.64	31.78	−0.14
60.00	2.99	40.53	40.62	−0.08
60.00	4.01	40.39	40.57	−0.18
60.00	5.10	40.39	40.54	−0.15
60.00	7.78	40.61	40.56	0.05
60.00	8.85	40.73	40.62	0.11
60.00	9.81	40.83	40.68	0.15
60.00	11.36	40.99	40.83	0.16
60.00	13.18	41.18	41.07	0.10

4. Experimental design, materials, and methods

The aqueous solutions were prepared using the following chemicals. Alfa Aesar (Netherlands) supplied anhydrous magnesium chloride (99.21 mass% of the main constituent as stated in the manufacturer's certificate). Methanol qualified as "chemically pure" (purity not less than 99.7 mass%) was purchased from Vekton (Russia). Deionized water with a resistivity of 18.2 MΩ·cm at 298 K was obtained in a lab via the Simplicity UV system (Merck Millipore, USA). Compressed high-purity methane (CH_4 fraction not less than 99.99 vol%) was delivered from the Moscow Gas Refinery (Moscow Region, Russia) in 40 L cylinders with a gas pressure of 15 MPa. Gas hydrate equilibrium measurements were performed using the GHA350 rig [18] manufactured by PSL Systemtechnik (Germany). The main part of the rig is a high-pressure vessel of Hastelloy C276 with

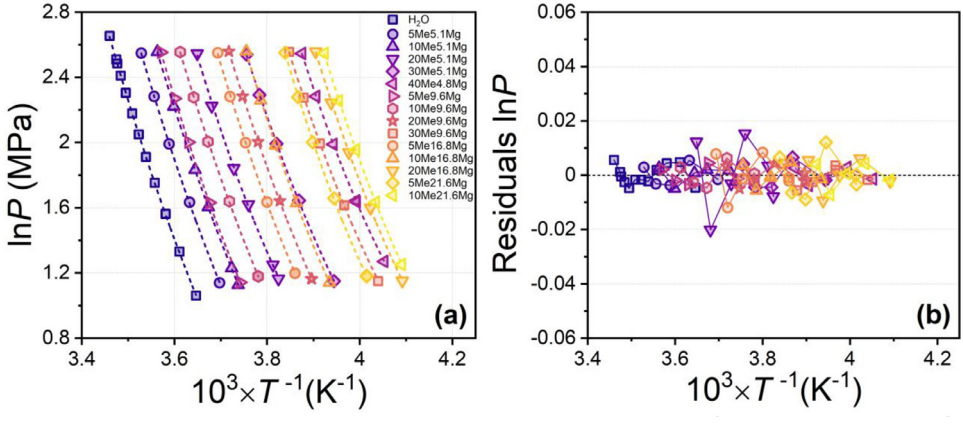

Fig. 8. **(a)** Measured methane hydrate equilibrium (V–L_w–H) points for the mixed system of CH_4–MeOH–$MgCl_2$–H_2O and approximations by three-parameter function $\ln P = A + B/T + C \cdot \ln T$ (color dashed lines, coefficients are in Table 3), the first number in the designation of the mixed sample is the concentration of MeOH, the second number is the concentration of $MgCl_2$ in mass%; **(b)** fitting residuals vs. independent variable of T^{-1}; the error bars are smaller than the symbol size.

Table 7
Results of surface fitting by empirical function 4 from ref. [13] of methane hydrate equilibrium temperature suppression ΔT_h vs. MeOH content in water solution in mol% scale and gas pressure for CH_4–MeOH–H_2O system (concatenated dataset of this work and from ref. [7,8]).

MeOH mol fraction, mol%	*P*, MPa	ΔT_h experiment, K	ΔT_h fit, K	Residuals of ΔT_h (experiment–fit), K
0	2.89	0	0	0
0	3.79	0	0	0
0	4.77	0	0	0
0	5.78	0	0	0
0	6.77	0	0	0
0	7.78	0	0	0
0	8.84	0	0	0
0	10.03	0	0	0
0	11.14	0	0	0
0	12.01	0	0	0
0	12.32	0	0	0
0	13.20	0	0	0
2.87	3.10	2.12	2.05	0.07
2.87	5.27	2.12	2.05	0.07
2.87	7.19	2.14	2.05	0.09
2.87	9.79	2.15	2.05	0.10
2.87	12.77	2.14	2.07	0.07
5.89	3.01	4.41	4.41	−0.00
5.89	5.05	4.42	4.40	0.02
5.89	5.99	4.43	4.40	0.03
5.89	6.90	4.44	4.40	0.04
5.89	7.45	4.44	4.40	0.04
5.89	8.19	4.44	4.40	0.04
5.89	9.82	4.46	4.42	0.04
5.89	12.79	4.48	4.45	0.03
12.32	2.99	9.86	9.93	−0.07
12.32	4.98	9.84	9.91	−0.07
12.32	5.99	9.84	9.91	−0.07
12.32	6.91	9.84	9.91	−0.07
12.32	7.43	9.84	9.91	−0.07
12.32	8.15	9.85	9.92	−0.07
12.32	10.37	9.88	9.96	−0.08
12.32	12.71	9.91	10.02	−0.11
19.43	2.95	16.58	16.38	0.21
19.43	4.90	16.41	16.35	0.06
19.43	5.94	16.37	16.34	0.03
19.43	7.01	16.36	16.35	0.01
19.43	7.50	16.36	16.35	0.01
19.43	8.14	16.36	16.36	−0.00
19.43	9.78	16.38	16.40	−0.02
19.43	12.75	16.45	16.53	−0.08
27.26	3.09	23.77	23.53	0.25
27.26	4.76	23.54	23.49	0.05
27.26	4.78	23.53	23.49	0.04
27.26	5.84	23.49	23.48	0.01
27.26	6.91	23.49	23.49	−0.00
27.26	6.93	23.49	23.49	−0.00
27.26	7.49	23.49	23.50	−0.01
27.26	8.35	23.51	23.52	−0.01
27.26	9.73	23.55	23.57	−0.02
27.26	9.77	23.55	23.57	−0.02
27.26	12.76	23.66	23.76	−0.10
31.23	5.09	27.14	27.08	0.07
31.23	7.29	27.15	27.08	0.06
31.23	9.98	27.18	27.18	−0.00
31.23	12.94	27.31	27.40	−0.09

(*continued on next page*)

Table 7 (*continued*)

MeOH mol fraction, mol%	*P*, MPa	ΔT_h experiment, K	ΔT_h fit, K	Residuals of ΔT_h (experiment–fit), K
35.98	2.98	31.53	31.43	0.09
35.98	5.03	31.38	31.37	0.01
35.98	5.93	31.36	31.37	−0.01
35.98	5.94	31.36	31.37	−0.01
35.98	6.90	31.35	31.38	−0.03
35.98	7.52	31.35	31.39	−0.03
35.98	7.53	31.35	31.39	−0.03
35.98	7.99	31.36	31.40	−0.04
35.98	9.76	31.43	31.48	−0.05
35.98	12.76	31.64	31.73	−0.09
45.75	2.99	40.53	40.63	−0.10
45.75	4.01	40.39	40.58	−0.20
45.75	5.10	40.39	40.55	−0.17
45.75	7.78	40.61	40.58	0.03
45.75	8.85	40.73	40.64	0.09
45.75	9.81	40.83	40.70	0.13
45.75	11.36	40.99	40.85	0.15
45.75	13.18	41.18	41.08	0.10

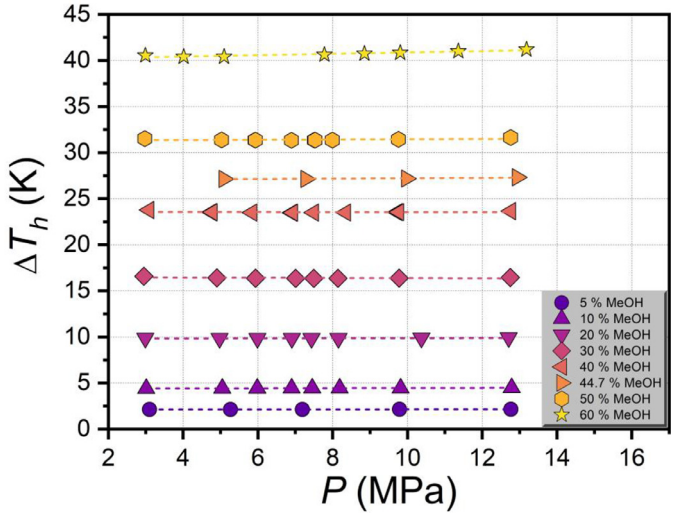

Fig. 9. Suppression of gas hydrate equilibrium temperature ΔT_h vs. equilibrium pressure in a system of CH_4–MeOH–H_2O; symbols – experimental points, dashed lines – linear fits; mass fraction of methanol in aqueous solution is shown in the legend; the error bars are smaller than the symbol size.

a volume of 600 cm^3, designed for a maximum pressure of 35 MPa in the temperature range of 230–310 K. The reactor is in the shape of a cylindrical vessel with a 0.085 m diameter. To measure the temperature and pressure of the fluids, the autoclave is equipped with a Pt100 resistance thermometer (maximum error ± 0.1 K) and a gauge pressure sensor coupled to a 700G30 precision electronic manometer (Fluke, USA) with a maximum error of ± 0.017 MPa. The Pt100 sensor is connected via a Lemo-connector to a liquid thermostat CC 505 or Ministat 240 (both Huber, Germany), which circulates ethanol (coolant) in the outer jacket of a high-pressure vessel for temperature control. To guarantee a high accuracy of measurement, the Pt100 sensor was calibrated before the experiments to 5 values equally distributed between 233 and 303 K with reference devices, including PRT 5616–12 (maximum error ± 0.011 K) and reference ther-

Table 8
Results of surface fitting by empirical function 4 from ref. [13] of methane hydrate equilibrium temperature suppression ΔT_h vs. $MgCl_2$ content in water solution in mass% scale and gas pressure for CH_4–$MgCl_2$–H_2O system.

$MgCl_2$ mass fraction, mass%	P, MPa	ΔT_h experiment, K	ΔT_h fit, K	Residuals of ΔT_h (experiment–fit), K
0	2.89	0	0	0
0	3.79	0	0	0
0	4.77	0	0	0
0	5.78	0	0	0
0	6.77	0	0	0
0	7.78	0	0	0
0	8.84	0	0	0
0	10.03	0	0	0
0	11.14	0	0	0
0	12.01	0	0	0
0	12.32	0	0	0
0	13.00	0	0	0
5.12	3.07	2.14	2.11	0.02
5.12	5.16	2.16	2.14	0.02
5.12	7.29	2.19	2.17	0.01
5.12	9.81	2.20	2.20	−0.00
5.12	12.80	2.18	2.23	−0.05
8.43	3.15	4.03	4.01	0.02
8.43	5.15	4.06	4.07	−0.01
8.43	7.33	4.13	4.13	0.01
8.43	9.77	4.19	4.18	0.01
8.43	12.58	4.21	4.23	−0.02
16.80	3.17	12.65	12.63	0.02
16.80	5.16	12.80	12.81	−0.01
16.80	7.33	12.98	12.98	0.00
16.80	9.82	13.15	13.15	−0.00
16.80	12.68	13.30	13.31	−0.01
22.28	3.04	23.33	23.26	0.07
22.28	5.16	23.65	23.61	0.04
22.28	7.26	23.89	23.92	−0.02
22.28	9.72	24.17	24.23	−0.06
22.28	12.99	24.54	24.56	−0.02
26.68[a]	3.17	36.19	36.23	−0.04
26.68[a]	5.11	36.66	36.72	−0.06
26.68[a]	6.86	37.15	37.13	0.02
26.68[a]	9.75	37.77	37.70	0.06
26.68[a]	12.91	38.21	38.21	0.01
26.68[a]	13.06	38.23	38.23	0.00

[a] Metastable equilibrium vapor – supercooled aqueous solution – gas hydrate (an aqueous solution of magnesium chloride is supercooled relative to the crystalline hydrate phase $MgCl_2 \cdot 12H_2O$). See Section 3.1 of the original research paper [1] for a more detailed discussion.

mometer 1524 (both Fluke, USA). Once the Pt100 was calibrated, its readings were verified by measuring the ice freezing point of deionized water, which was found to be 273.160 ± 0.013 K. This is the mean temperature and standard deviation at the ice crystallization plateau for 5 min, calculated from 146 points. The GHA350 gauge pressure sensor was calibrated to 2 points (0 MPa (ambient P) and 15 MPa) using a 717 5000 G calibrator (Fluke, USA). The procedure for subsequent verification of pressure sensor readings is outlined in ref. [19]. Intensive mixing of the fluids during the experiment is achieved with a Hei-TORQUE 400 Precision overhead motor (Heidolph, Germany), a magnetic coupling (Premex, Switzerland), and a shaft with a four-blade impeller. The blade height is 0.02 m and the diameter is 0.061 m. The blades are positioned 0.005 m from the bottom of the reactor. The height of the liquid layer in the reactor is 0.06 m for a sample volume of 300 mL.

The original research paper describes ramp and step heating techniques for hydrate equilibrium measurements [1]. Their applicability to different systems is analyzed in our recent work

Table 9
Results of surface fitting by empirical function 4 from ref. [13] of methane hydrate equilibrium temperature suppression ΔT_h vs. $MgCl_2$ content in water solution in mol% scale and gas pressure for CH_4–$MgCl_2$–H_2O system.

$MgCl_2$ mol fraction, mol%	*P*, MPa	ΔT_h experiment, K	ΔT_h fit, K	Residuals of ΔT_h (experiment–fit), K
0	2.89	0	0	0
0	3.79	0	0	0
0	4.77	0	0	0
0	5.78	0	0	0
0	6.77	0	0	0
0	7.78	0	0	0
0	8.84	0	0	0
0	10.03	0	0	0
0	11.14	0	0	0
0	12.01	0	0	0
0	12.32	0	0	0
0	13.00	0	0	0
1.01	3.07	2.14	2.11	0.02
1.01	5.16	2.16	2.14	0.01
1.01	7.29	2.19	2.17	0.01
1.01	9.81	2.20	2.20	−0.01
1.01	12.80	2.18	2.23	−0.05
1.71	3.15	4.03	4.01	0.02
1.71	5.15	4.06	4.07	−0.01
1.71	7.33	4.13	4.13	0.01
1.71	9.77	4.19	4.18	0.01
1.71	12.58	4.21	4.23	−0.02
3.68	3.17	12.65	12.63	0.02
3.68	5.16	12.80	12.81	−0.01
3.68	7.33	12.98	12.98	0.00
3.68	9.82	13.15	13.15	−0.00
3.68	12.68	13.30	13.31	−0.01
5.15	3.04	23.33	23.26	0.07
5.15	5.16	23.65	23.61	0.04
5.15	7.26	23.89	23.92	−0.02
5.15	9.72	24.17	24.23	−0.06
5.15	12.99	24.54	24.56	−0.02
6.44[a]	3.17	36.19	36.23	−0.04
6.44[a]	5.11	36.66	36.72	−0.06
6.44[a]	6.86	37.15	37.13	0.02
6.44[a]	9.75	37.77	37.70	0.06
6.44[a]	12.91	38.21	38.21	0.01
6.44[a]	13.06	38.23	38.23	0.00

[a] Metastable equilibrium vapor – supercooled aqueous solution – gas hydrate (an aqueous solution of magnesium chloride is supercooled relative to the crystalline hydrate phase $MgCl_2 \cdot 12H_2O$). See Section 3.1 of the original research paper [1] for a more detailed discussion.

[20]. Figs. 14 and 15 are examples of experimental pressure and temperature curves obtained using the ramp heating technique (0.1 K/h) and the step heating technique to measure the three-phase gas–aqueous solution–gas hydrate equilibrium in the presence of 10Me16.8Mg and 26.7Mg aqueous solution samples, respectively. Each aqueous inhibitor solution was prepared gravimetrically. The mixing masses of the components were monitored using a PA413C balance (Ohaus, USA). This balance has a resolution of 0.001 g and a maximum error of no more than ± 0.01 g. An aqueous solution of 300 mL was placed in an autoclave at 295 K. The air was evacuated from the empty volume of the autoclave by purging it three times with working gas (methane). The autoclave was then pressurized with methane to a preset pressure, stirring at 600 rpm. The Reynolds numbers of the samples tested are in the range of $9 \cdot 10^3$–$3.7 \cdot 10^4$ at 293.15 K (see Fig. 1 and description in section 2 in [1]). The ramp heating technique (0.1 K/h) was primarily used to measure the equilibrium points. For some solution samples, preliminary experiments were performed at a higher heating rate of 0.5 K/h (see Table 1). For concentrated magnesium

Table 10
Measured ice freezing points T_{ice} at 0.1 MPa for aqueous solutions of MeOH, $MgCl_2$, and MeOH+$MgCl_2$; each given value corresponds to a single ice freezing point measurement.

Sample #	Aqueous solution sample	ω_{MeOH}, mass%	ω_{MgCl2}, mass%	Point #	T_{ice} / °C	T_{ice} / K	ΔT_{ice} / K
1	H_2O	0	0	1	0.00	273.15	0.00
2	5Me	5.00	0	2	−3.11	270.04	3.11
				3	−3.11	270.04	3.11
				4	−3.10	270.05	3.10
				5	−3.10	270.05	3.10
3	10Me	10.01	0	6	−6.56	266.59	6.56
				7	−6.59	266.56	6.59
4	20Me	20.00	0	8	−15.42	257.73	15.42
				9	−15.49	257.66	15.49
				10	−15.48	257.67	15.48
5	30Me	30.01	0	11	−26.95	246.20	26.95
6	40Me	39.99	0	12	−40.03	233.12	40.03
7	50Me	49.99	0	13	−55.54	217.61	55.54
				14	−55.55	217.60	55.55
8	2.4Mg	0	2.40	15	−1.31	271.84	1.31
				16	−1.31	271.84	1.31
9	5.1Mg	0	5.13	17	−3.05	270.10	3.05
				18	−3.05	270.10	3.05
10	8.4Mg	0	8.42	19	−5.92	267.23	5.92
				20	−5.89	267.26	5.89
11	12.3Mg	0	12.30	21	−10.68	262.47	10.68
				22	−10.68	262.47	10.68
12	16.8Mg	0	16.80	23	−19.13	254.02	19.13
				24	−19.13	254.02	19.13
13	22.4Mg	0	22.40	25	−35.92[a]	237.23[a]	35.92[a]
				26	−35.89[a]	237.26[a]	35.89[a]
14	5Me5.1Mg	5.00	5.13	27	−6.70	266.45	6.70
				28	−6.70	266.45	6.70
15	10Me5.1Mg	10.01	5.14	29	−11.18	261.97	11.18
				30	−11.11	262.04	11.11
16	20Me5.1Mg	19.99	5.13	31	−21.57	251.58	21.57
				32	−21.57	251.58	21.57
17	30Me5.1Mg	30.00	5.13	33	−35.50	237.65	35.50
18	40Me4.8Mg	40.00	4.80	34	−49.24	223.91	49.24
				35	−49.29	223.86	49.29
19	5Me9.6Mg	5.00	9.63	36	−11.77	261.38	11.77
				37	−11.75	261.40	11.75
20	10Me9.6Mg	10.00	9.63	38	−16.70	256.45	16.70
				39	−16.71	256.44	16.71
21	20Me9.6Mg	20.00	9.63	40	−29.25	243.90	29.25
				41	−29.28	243.87	29.28
22	30Me9.6Mg	30.00	9.62	42	−45.05	228.10	45.05
				43	−45.04	228.11	45.04
23	5Me16.8Mg	5.00	16.81	44	−24.02	249.13	24.02
				45	−24.02	249.13	24.02
24	10Me16.8Mg	10.00	16.81	46	−31.32	241.83	31.32
				47	−31.32	241.83	31.32
25	20Me16.8Mg	20.00	16.80	48	−49.29	223.86	49.29
				49	−49.33	223.82	49.33
26	5Me21.6Mg	5.00	21.60	50	−39.47	233.68	39.47
				51	−39.47	233.68	39.47
27	10Me21.6Mg	10.00	21.60	52	−49.42	223.73	49.42
				53	−49.52	223.63	49.52

[a] Metastable equilibrium aqueous $MgCl_2$ solution – ice. See Section 3.5 of the original research paper [1] for a more detailed discussion.

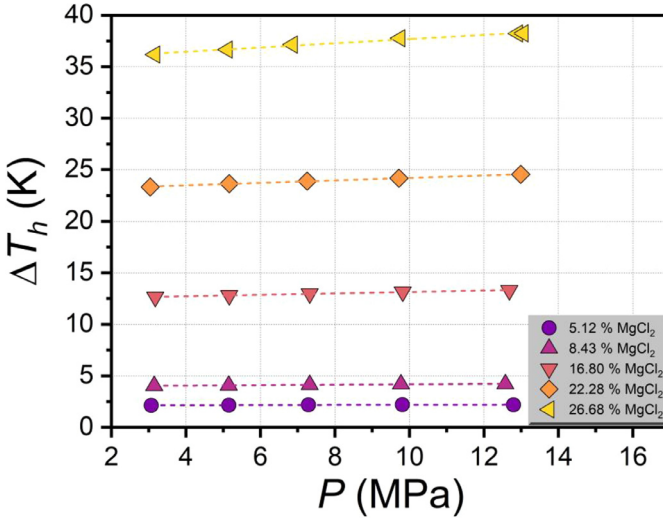

Fig. 10. Suppression of gas hydrate equilibrium temperature ΔT_h vs. equilibrium pressure in a system of CH_4–$MgCl_2$–H_2O; symbols – experimental points, dashed lines – linear fits; mass fraction of $MgCl_2$ in aqueous solution is shown in the legend; the error bars are smaller than the symbol size.

chloride solutions (22.28 and 26.68 mass%) and methanol solution (60.00 mass%), equilibrium conditions were also determined using a step heating technique (0.1 K step with 3 h hold time before hydrate dissociation endpoint and 0.2 K step with 1 h hold time after hydrate dissociation endpoint). The endpoint of methane hydrate dissociation was considered to be the equilibrium point. Its coordinates were determined by linear approximation of the two segments of the *P-T* trajectory (before and after complete hydrate decomposition) and by finding the intersection of the two linear functions.

The ice freezing point of each aqueous solution was measured in an 80 mL double-walled glass cell and stirred on a magnetic stirrer at 600 rpm. The sample temperature was controlled by a calibrated PRT 5622–10-P quick-response probe combined with a 1524 reference thermometer (both Fluke, USA). This combination allows the temperature to be measured with an error of no more than ± 0.04 K. Ethanol was circulated between two glass walls of the cell using an F81-ME cryostat (Julabo, Germany). The temperature at the plateau (or maximum) after ice nucleation in the supercooled aqueous solution was assigned as the ice freezing point. Details of the technique are described elsewhere [13]. Two consecutive measurements were performed on each sample to achieve repeatability of ice freezing point ≤ 0.1 K.

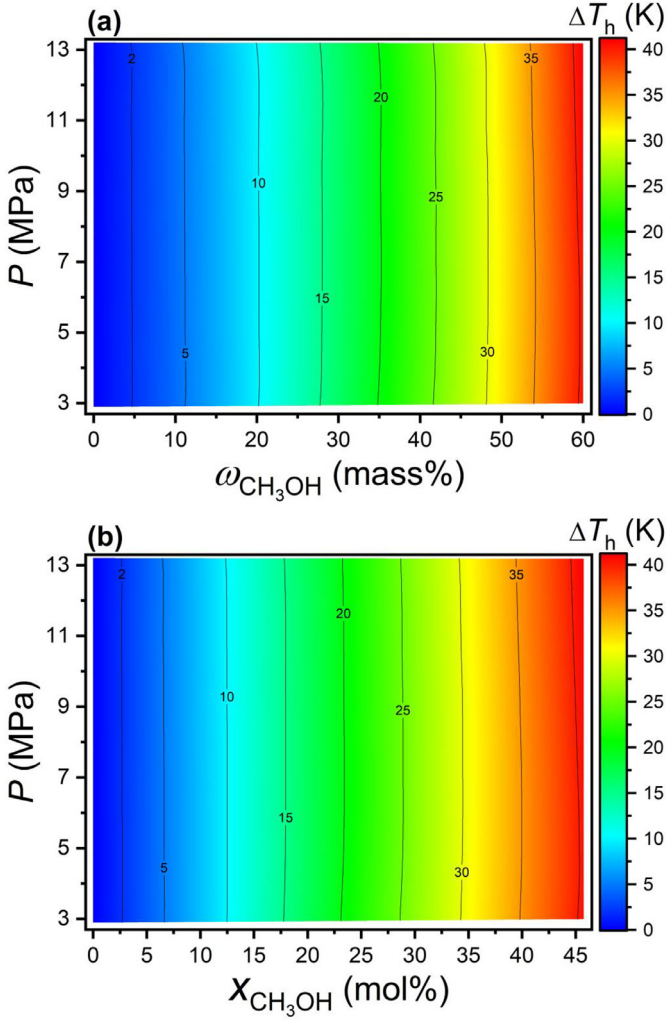

Fig. 11. Color contours with isolines of hydrate equilibrium temperature suppression ΔT_h in a system of CH_4–MeOH–H_2O for the entire range of pressure (3–13 MPa) and methanol concentrations **(a)** in mass%, **(b)** in mol%.

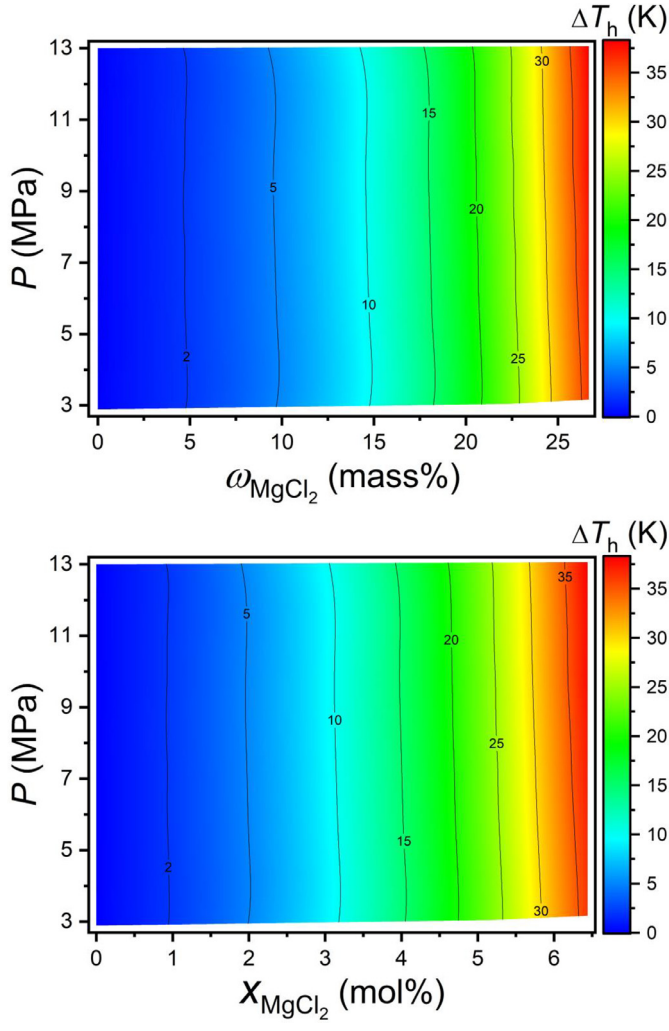

Fig. 12. Color contours with isolines of hydrate equilibrium temperature suppression ΔT_h in a system of CH_4–$MgCl_2$–H_2O for the entire range of pressure (3–13 MPa) and salt concentrations; (upper panel) in mass%, (lower panel) in mol%.

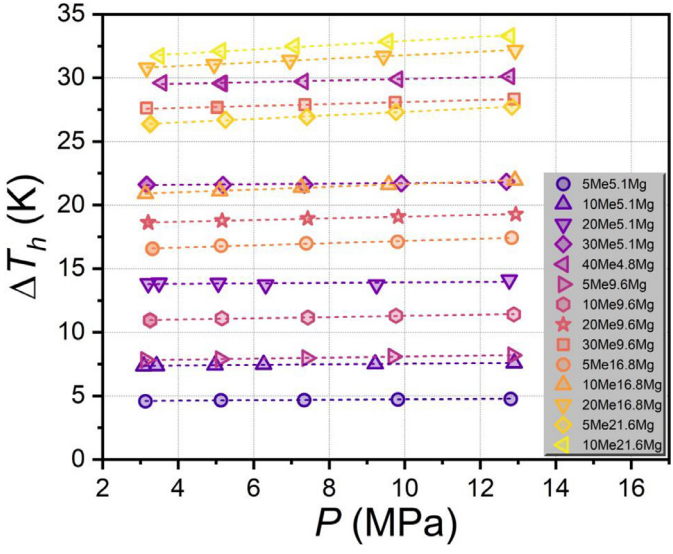

Fig. 13. Suppression of gas hydrate equilibrium temperature ΔT_h vs. equilibrium pressure in the mixed system of CH_4–MeOH–$MgCl_2$–H_2O; symbols – experimental points, dashed lines – linear fits; the first number in the designation of the mixed sample is the concentration of MeOH, the second number is the concentration of $MgCl_2$ in mass%; the error bars are smaller than the symbol size.

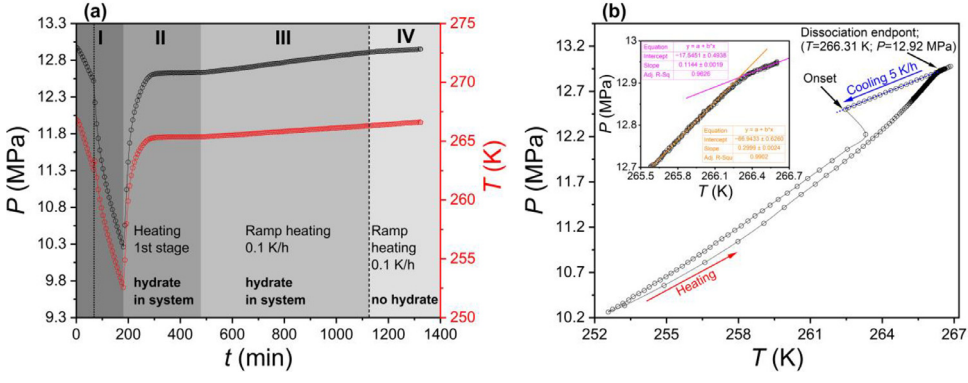

Fig. 14. **(a)** The pressure and temperature experimental curves for the CH_4–MeOH–$MgCl_2$–H_2O system obtained by measuring the three-phase gas–water solution–gas hydrate equilibrium (mixed solution sample 10Me16.8Mg, equilibrium point #146 in Table 1) with the ramp heating technique (0.1 K/h); the methane hydrate onset and the methane hydrate dissociation endpoint are indicated by the dotted and dashed lines; **(b)** the obtained *P-T* trajectory.

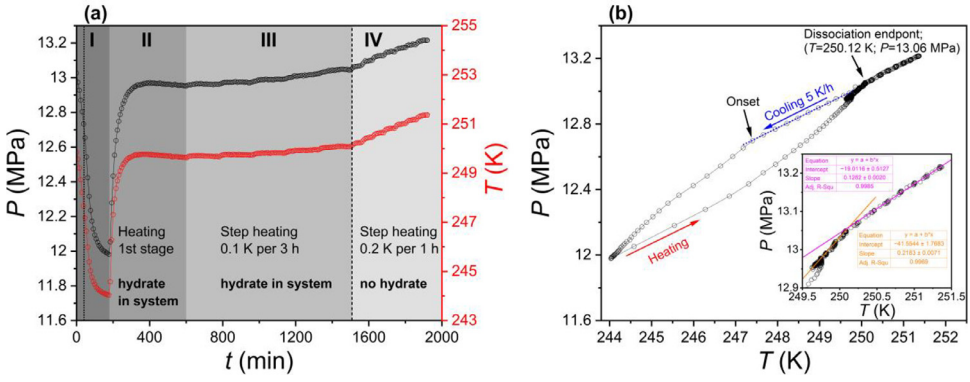

Fig. 15. **(a)** The pressure and temperature experimental curves for the CH_4–$MgCl_2$–H_2O system obtained by measuring the three-phase gas–water solution–gas hydrate equilibrium (sample 26.7Mg, equilibrium point #81 in Table 1) with the step heating technique; the methane hydrate onset and the methane hydrate dissociation endpoint are indicated by the dotted and dashed lines; **(b)** the obtained *P*-*T* trajectory.

Table 11
Parameters of approximation by linear function $\Delta T_h/(T_0 T) = a + b \cdot T$ of experimental points in the range of 3–13 MPa for systems of CH_4–MeOH–H_2O (concatenated dataset of this work and from [7,8]), CH_4–$MgCl_2$–H_2O (data of this work), CH_4–MeOH–$MgCl_2$–H_2O (data of this work).

#	Aqueous solution sample	*a*, K^{-1}		*b*, K^{-2}		Adjusted R^2	ANOVA for Slope value[a]
		Value	Standard Error	Value	Standard Error		
1	H_2O	n/a	n/a	n/a	n/a	n/a	n/a
2	5Me	$7.31 \cdot 10^{-5}$	$4.73 \cdot 10^{-6}$	$-1.64 \cdot 10^{-7}$	$1.69 \cdot 10^{-8}$	0.9592	+
3	10Me	$1.52 \cdot 10^{-4}$	$4.73 \cdot 10^{-6}$	$-3.43 \cdot 10^{-7}$	$1.70 \cdot 10^{-8}$	0.9830	+
4	20Me	$3.72 \cdot 10^{-4}$	$1.15 \cdot 10^{-5}$	$-8.95 \cdot 10^{-7}$	$4.23 \cdot 10^{-8}$	0.9846	+
5	30Me	$6.89 \cdot 10^{-4}$	$2.48 \cdot 10^{-5}$	$-1.77 \cdot 10^{-6}$	$9.31 \cdot 10^{-8}$	0.9809	+
6	40Me	$9.78 \cdot 10^{-4}$	$3.07 \cdot 10^{-5}$	$-2.53 \cdot 10^{-6}$	$1.18 \cdot 10^{-7}$	0.9785	+
7	44.7Me	$1.02 \cdot 10^{-3}$	$3.46 \cdot 10^{-5}$	$-2.54 \cdot 10^{-6}$	$1.35 \cdot 10^{-7}$	0.9916	+
8	50Me	$1.29 \cdot 10^{-3}$	$3.91 \cdot 10^{-5}$	$-3.36 \cdot 10^{-6}$	$1.56 \cdot 10^{-7}$	0.9810	+
9	60Me	$1.57 \cdot 10^{-3}$	$5.32 \cdot 10^{-5}$	$-4.01 \cdot 10^{-6}$	$2.20 \cdot 10^{-7}$	0.9794	+
10	5.1Mg	$6.75 \cdot 10^{-5}$	$4.97 \cdot 10^{-6}$	$-1.43 \cdot 10^{-7}$	$1.77 \cdot 10^{-8}$	0.9413	+
11	8.4Mg	$1.04 \cdot 10^{-4}$	$8.38 \cdot 10^{-6}$	$-1.85 \cdot 10^{-7}$	$3.01 \cdot 10^{-8}$	0.9017	+
12	16.8Mg	$3.26 \cdot 10^{-4}$	$2.11 \cdot 10^{-5}$	$-5.76 \cdot 10^{-7}$	$7.83 \cdot 10^{-8}$	0.9300	+
13	22.3Mg	$6.54 \cdot 10^{-4}$	$4.37 \cdot 10^{-5}$	$-1.26 \cdot 10^{-6}$	$1.69 \cdot 10^{-7}$	0.9319	+
14	26.7Mg[b]	$9.56 \cdot 10^{-4}$	$5.51 \cdot 10^{-5}$	$-1.71 \cdot 10^{-6}$	$2.24 \cdot 10^{-7}$	0.9197	+
15	5Me5.1Mg	$1.33 \cdot 10^{-4}$	$5.73 \cdot 10^{-6}$	$-2.62 \cdot 10^{-7}$	$2.06 \cdot 10^{-8}$	0.9757	+
16	10Me5.1Mg	$2.28 \cdot 10^{-4}$	$4.18 \cdot 10^{-6}$	$-4.80 \cdot 10^{-7}$	$1.53 \cdot 10^{-8}$	0.9949	+
17	20Me5.1Mg	$5.14 \cdot 10^{-4}$	$4.45 \cdot 10^{-5}$	$-1.23 \cdot 10^{-6}$	$1.67 \cdot 10^{-7}$	0.9149	+
18	30Me5.1Mg	$8.24 \cdot 10^{-4}$	$2.40 \cdot 10^{-5}$	$-2.03 \cdot 10^{-6}$	$9.23 \cdot 10^{-8}$	0.9898	+
19	40Me4.8Mg	$1.06 \cdot 10^{-3}$	$4.63 \cdot 10^{-5}$	$-2.55 \cdot 10^{-6}$	$1.83 \cdot 10^{-7}$	0.9747	+
20	5Me9.6Mg	$2.09 \cdot 10^{-4}$	$1.66 \cdot 10^{-5}$	$-3.85 \cdot 10^{-7}$	$6.05 \cdot 10^{-8}$	0.9079	+
21	10Me9.6Mg	$3.12 \cdot 10^{-4}$	$9.90 \cdot 10^{-6}$	$-6.13 \cdot 10^{-7}$	$3.66 \cdot 10^{-8}$	0.9824	+
22	20Me9.6Mg	$5.86 \cdot 10^{-4}$	$1.69 \cdot 10^{-5}$	$-1.26 \cdot 10^{-6}$	$6.44 \cdot 10^{-8}$	0.9870	+
23	30Me9.6Mg	$9.45 \cdot 10^{-4}$	$4.19 \cdot 10^{-5}$	$-2.19 \cdot 10^{-6}$	$1.65 \cdot 10^{-7}$	0.9722	+
24	5Me16.8Mg	$4.46 \cdot 10^{-4}$	$2.19 \cdot 10^{-5}$	$-8.28 \cdot 10^{-7}$	$8.29 \cdot 10^{-8}$	0.9518	+
25	10Me16.8Mg	$5.78 \cdot 10^{-4}$	$3.71 \cdot 10^{-5}$	$-1.10 \cdot 10^{-6}$	$1.42 \cdot 10^{-7}$	0.9223	+
26	20Me16.8Mg	$9.24 \cdot 10^{-4}$	$5.19 \cdot 10^{-5}$	$-1.91 \cdot 10^{-6}$	$2.07 \cdot 10^{-7}$	0.9549	+
27	5Me21.6Mg	$7.48 \cdot 10^{-4}$	$4.52 \cdot 10^{-5}$	$-1.46 \cdot 10^{-6}$	$1.77 \cdot 10^{-7}$	0.9305	+
28	10Me21.6Mg	$8.62 \cdot 10^{-4}$	$3.24 \cdot 10^{-5}$	$-1.61 \cdot 10^{-6}$	$1.30 \cdot 10^{-7}$	0.9745	+

[a] + means the slope value is significantly different from 0 at the 0.05 level based on the analysis of variance. This indicates a statistically meaningful dependence of $\Delta T_h/(T_0 T)$ on T for all inhibited systems of this work.

[b] Metastable equilibrium vapor – supercooled aqueous solution – gas hydrate (an aqueous solution of magnesium chloride is supercooled relative to the crystalline hydrate phase $MgCl_2 \cdot 12H_2O$). See Section 3.1 of the original research paper [1] for a more detailed discussion.

Limitations

Not applicable.

Ethics Statements

The studies described in the manuscript adhered to Ethics in publishing standards (https://www.elsevier.com/journals/data-in-brief/2352–3409/guide-for-authors) and did not involve human or animal subjects.

Data Availability

Raw data of gas hydrate equilibrium measurements for CH4 – MeOH – MgCl2 – H2O system and ice freezing point determination of aqueous MeOH and MgCl2 solutions (Original data) (Mendeley Data)

CRediT Author Statement

Anton P. Semenov: Data curation, Visualization, Writing – original draft, Validation, Writing – review & editing, Project administration, Funding acquisition; **Rais I. Mendgaziev:** Investigation, Data curation; **Vladimir A. Istomin:** Writing – review & editing; **Daria V. Sergeeva:** Writing – review & editing; **Vladimir A. Vinokurov:** Resources, Supervision, Writing – review & editing; **Yinghua Gong:** Investigation; **Tianduo Li:** Supervision, Funding acquisition, Writing – review & editing; **Andrey S. Stoporev:** Validation, Writing – original draft, Writing – review & editing.

Acknowledgments

Methane hydrate equilibrium studies were supported by the Russian Science Foundation (grant 20–79–10377). Assessment of the economic efficiency of gas hydrate inhibitors was supported by the Program for Scientific Research Innovation Team in Colleges and Universities of Shandong Province of Qilu University of Technology (Shandong Academy of Sciences).

Declaration of Competing Interest

The authors declare that they have no known competing financial interests or personal relationships that could have appeared to influence the work reported in this paper.

References

[1] A.P. Semenov, R.I. Mendgaziev, V.A. Istomin, D.V. Sergeeva, V.A. Vinokurov, Y. Gong, T. Li, A.S. Stoporev, Searching for synergy between alcohol and salt to produce more potent and environmentally benign gas hydrate inhibitors, Chem. Eng. Sci. 283 (2024) 119361, doi:10.1016/j.ces.2023.119361.
[2] A.P. Semenov, R.I. Mendgaziev, A.S. Stoporev, Y.F. Gushchina, B.M. Anikushin, P.A. Gushchin, V.N. Khlebnikov, Synergism of methanol and magnesium chloride for thermodynamic inhibition of methane hydrate, Chem. Technol. Fuels Oils. 54 (2019) 738–742, doi:10.1007/s10553-019-00981-2.
[3] H.J. Ng, D.B. Robinson, Hydrate formation in systems containing methane, ethane, propane, carbon dioxide or hydrogen sulfide in the presence of methanol, Fluid Phase Equilib 21 (1985) 145–155, doi:10.1016/0378-3812(85)90065-2.
[4] D.B. Robinson, H.J. Ng, Hydrate formation and inhibition in gas or gas condensate streams, J. Can. Pet. Technol. 25 (1986) 26–30, doi:10.2118/86-04-01.

[5] H. Haghighi, A. Chapoy, R. Burgess, S. Mazloum, B. Tohidi, Phase equilibria for petroleum reservoir fluids containing water and aqueous methanol solutions: experimental measurements and modelling using the CPA equation of state, Fluid Phase Equilib 278 (2009) 109–116, doi:10.1016/j.fluid.2009.01.009.
[6] A.H. Mohammadi, D. Richon, Phase equilibria of methane hydrates in the presence of methanol and/or ethylene glycol aqueous solutions, Ind. Eng. Chem. Res. 49 (2010) 925–928, doi:10.1021/ie901357m.
[7] A.P. Semenov, Y. Gong, V.I. Medvedev, A.S. Stoporev, V.A. Istomin, V.A. Vinokurov, T. Li, Dataset for the new insights into methane hydrate inhibition with blends of vinyl lactam polymer and methanol, monoethylene glycol, or diethylene glycol as hybrid inhibitors, Data Br. 46 (2023) 108892. https://doi.org/10.1016/j.dib.2023.108892.
[8] A.P. Semenov, Y. Gong, V.I. Medvedev, A.S. Stoporev, V.A. Istomin, V.A. Vinokurov, T. Li, New insights into methane hydrate inhibition with blends of vinyl lactam polymer and methanol, monoethylene glycol, or diethylene glycol as hybrid inhibitors, Chem. Eng. Sci. 268 (2023) 118387, doi:10.1016/j.ces.2022.118387.
[9] S.P. Kang, M.K. Chun, H. Lee, Phase equilibria of methane and carbon dioxide hydrates in the aqueous MgCl2 solutions, Fluid Phase Equilib 147 (1998) 229–238, doi:10.1016/S0378-3812(98)00233-7.
[10] Z. Atik, C. Windmeier, L.R. Oellrich, Experimental gas hydrate dissociation pressures for pure methane in aqueous solutions of MgCl 2 and CaCl 2 and for a (Methane + Ethane) gas mixture in an aqueous solution of (NaCl + MgCl 2), J. Chem. Eng. Data. 51 (2006) 1862–1867, doi:10.1021/je060225a.
[11] A.H. Mohammadi, I. Kraouti, D. Richon, Methane hydrate phase equilibrium in the presence of NaBr, KBr, CaBr2, K2CO3, and MgCl2 aqueous solutions: experimental measurements and predictions of dissociation conditions, J. Chem. Thermodyn. 41 (2009) 779–782, doi:10.1016/j.jct.2009.01.004.
[12] N.A. Sami, K. Das, J.S. Sangwai, N. Balasubramanian, Phase equilibria of methane and carbon dioxide clathrate hydrates in the presence of (methanol+MgCl2) and (ethylene glycol+MgCl2) aqueous solutions, J. Chem. Thermodyn. 65 (2013) 198–203, doi:10.1016/j.jct.2013.05.050.
[13] A.P. Semenov, R.I. Mendgaziev, A.S. Stoporev, V.A. Istomin, D.V. Sergeeva, A.G. Ogienko, V.A. Vinokurov, The pursuit of a more powerful thermodynamic hydrate inhibitor than methanol. Dimethyl sulfoxide as a case study, Chem. Eng. J. (2021) 130227, doi:10.1016/j.cej.2021.130227.
[14] H.F. Gibbard, A.F. Gossmann, Freezing points of electrolyte mixtures. I. Mixtures of sodium chloride and magnesium chloride in water, J. Solution Chem. 3 (1974) 385–393, doi:10.1007/BF00646479.
[15] F.H. Conrad, E.F. Hill, E.A. Ballman, Freezing points of the system ethylene glycol-methanol-water, Ind. Eng. Chem. 32 (1940) 542–543, doi:10.1021/ie50364a023.
[16] H.K. Ross, Cryoscopic studies - concentrated solutions of hydroxy compounds, Ind. Eng. Chem. 46 (1954) 601–610, doi:10.1021/ie50531a054.
[17] Y. Hu, J.H. Sa, B.R. Lee, A.K. Sum, Universal correlation for gas hydrates suppression temperature of inhibited systems: III. salts and organic inhibitors, AIChE J 64 (2018) 4097–4109, doi:10.1002/aic.16369.
[18] A.P. Semenov, V.I. Medvedev, P.A. Gushchin, M.S. Kotelev, V.S. Yakushev, A.S. Stoporev, A.A. Sizikov, A.G. Ogienko, V.A. Vinokurov, Phase equilibrium for clathrate hydrate formed in methane + water + ethylene carbonate system, Fluid Phase Equilib 432 (2017) 1–9, doi:10.1016/j.fluid.2016.10.015.
[19] Y. Gong, R.I. Mendgaziev, W. Hu, Y. Li, Z. Li, A.S. Stoporev, A. Yu. Manakov, V.A. Vinokurov, T. Li, A.P. Semenov, Urea as a green thermodynamic inhibitor of sII gas hydrates, Chem. Eng. J. (2022) 132386, doi:10.1016/j.cej.2021.132386.
[20] A.P. Semenov, R.I. Mendgaziev, T.B. Tulegenov, A.S. Stoporev, Analysis of the techniques for measuring the equilibrium conditions of gas hydrates formation, Chem. Technol. Fuels Oils. 58 (2022) 628–636, doi:10.1007/s10553-022-01429-w.